Localized excitations in (2+1)-dimensional systems

Xiao-yan Tang,[1] Sen-yue Lou,[1,2,3,4] and Ying Zhang[4]
[1]*Physics Department of Shanghai Jiao Tong University, Shanghai 200030, People's Republic of China*
[2] *CCAST (World Laboratory), P.O. Box 8730, Beijing 100080, People's Republic 0f China*
[3]*Department of Physics, Ningbo University, Ningbo 315211, People's Republic of China*
[4]*Abdus Salam International Centre for Theoretical Physics, Trieste, Italy*
(Received 15 May 2002; published 1 October 2002)

By means of a special variable separation approach, a common formula with some arbitrary functions has been obtained for some suitable physical quantities of various (2+1)-dimensional models such as the Davey-Stewartson (DS) model, the Nizhnik-Novikov-Veselov (NNV) system, asymmetric NNV equation, asymmetric DS equation, dispersive long wave equation, Broer-Kaup-Kupershmidt system, long wave–short wave interaction model, Maccari system, and a general $(N+M)$-component Ablowitz-Kaup-Newell-Segur (AKNS) system. Selecting the arbitrary functions appropriately, one may obtain abundant stable localized interesting excitations such as the multidromions, lumps, ring soliton solutions, breathers, instantons, etc. It is shown that some types of lower dimensional chaotic patterns such as the chaotic-chaotic patterns, periodic-chaotic patterns, chaotic line soliton patterns, chaotic dromion patterns, fractal lump patterns, and fractal dromion patterns may be found in higher dimensional soliton systems. The interactions between the traveling ring type soliton solutions are completely elastic. The traveling ring solitons pass through each other and preserve their shapes, velocities, and phases. Some types of localized weak solutions, peakons, are also discussed. Especially, the interactions between two peakons are not completely elastic. After the interactions, the traveling peakons also pass through each other and preserve their velocities and phases, however, they completely exchange their shapes.

DOI: 10.1103/PhysRevE.66.046601 PACS number(s): 05.45.Yv, 02.30.Ik

I. INTRODUCTION

In the past three decades, the solitons [1], chaos [2], and fractals [3] have been widely studied and applied in many natural sciences such as biology, chemistry, mathematics, communication, and especially in almost all branches of physics such as condensed matter physics, field theory, fluid dynamics, plasma physics, and optics. Usually, one considers that the solitons are the basic excitations of the integrable models while the chaos and fractals are the basic behaviors of the nonintegrable models. Actually, the above consideration may not be complete especially in higher dimensions. When saying that a model is integrable, one should emphasize two important facts. The first one is that we should point out under what special meaning(s) the model is integrable. For instance, we say a model is Painlevé integrable if it possesses the Painlevé property and a model is Lax or IST (inverse scattering transformation) integrable if it has a Lax pair and then can be solved by the IST approach. A model integrable under some special meanings may not be integrable under other meanings. For instance, some Lax integrable models may not be Painlevé integrable [4,5]. The second fact is that for the general solution of a higher dimensional integrable model, say, a Painlevé integrable model, there exist some characteristic, lower dimensional *arbitrary* functions. That means any lower dimensional chaotic and/or fractal solutions can be used to construct exact solutions of higher dimensional integrable models. In other words, any exotic behavior may propagate along the characteristics.

Solving nonlinear mathematical physics problems is much more difficult than solving the linear ones. In linear physics, the Fourier transformation method and the variable separation approach (VSA) are two most important approaches to find the exact solutions. It is known that the famous IST can be considered as an extension of the Fourier transformation in nonlinear physics. However, it is difficult to extend the VSA to nonlinear physics. Recently, two kinds of "variable separation" procedures have been established. The first method is called the "formal variable separation approach" (FVSA) [6], or equivalently the symmetry constraints [7] or nonlinearization of the Lax pairs [8]. The independent variables of a reduced field in FVSA have not been totally separated though the reduced field satisfies some lower-dimensional equations. The second type of variable separation method established first for the DS (Davey-Stewartson) equation in 1996 [9]. The method has been revisited and developed recently for various (2+1)-dimensional models like the NNV (Nizhnik-Novikov-Veselov) equation [10], ANNV (asymmetric NNV) equation [11], DS equation [12], ADS (asymmetric DS) equation [13], dispersive long wave equation (DLWE) [14], BKK (Broer-Kaup-Kupershmidt) system [15], a nonintegrable (2+1)-dimensional Kortweg–de Vries equation [16], long wave–short wave (LWSW) interaction model [17], Maccari system [18], and a general $(N+M)$-component Ablowitz-Kaup-Newell-Segur (AKNS) system [19]. After some slight modifications, one can find that there exists a common formula,

$$U\equiv\frac{-2\Delta q_y p_x}{(a_0+a_1p+a_2q+a_3pq)^2},\quad \Delta\equiv a_0a_3-a_1a_2, \tag{1.1}$$

to describe suitable physical quantities for all the models mentioned above. In Eq. (1.1), a_0, a_1, a_2, and a_3 are arbitrary constants and p is an arbitrary function of $\{x,t\}$ for all of them, while q of Eq. (1.1) may be an arbitrary function of $\{y,t\}$ for some models like the DS and NNV equations or an arbitrary solution of a Riccati equation for others (see following for details). Because some arbitrary characteristics, lower dimensional functions (like p), have been included in the universal formula (1.1), by selecting them appropriately, abundant stable localized structures have been revealed for these models. If we consider the boundary (or initial) conditions of the given localized excitations, we can find that all the (2+1)-dimensional localized solutions of these models are caused by the suitable boundary (or initial) conditions. In other words, the richness of the localized excitations of the (2+1)-dimensional models results from the fact that arbitrary exotic behaviors can propagate along some special characteristics of the models. In a previous study [20], we had pointed out that some types of nonlocalized chaotic and periodic patterns may exist also in (2+1)-dimensional soliton systems because of some arbitrary characteristic functions that can be included in the special variable separation solutions. In this paper, we mainly focus on the possibilities of the chaotic and fractal localized excitations and the interaction properties of some special types of localized excitations for the (2+1)-dimensional soliton systems.

For completeness, we review the variable separation approach for the DS system in Sec. II, list the known models that can be solved by means of the special variable separation approach in Sec. III, and give out some special types of stable localized excitations in Sec. IV. The completely elastic interaction property between two special ring solitons is also discussed in Sec. IV. In Secs. V and VI, we discuss the possible chaotic and fractal patterns for (2+1)-dimensional models, respectively. In Sec. VII, a special type of weak solution (peakons) and their noncompletely elastic interaction behavior are studied. The last section contains a summary and discussions.

II. VARIABLE SEPARATION APPROACH FOR THE DAVEY-STEWARTSON EQUATION

In order to establish a concrete variable separation procedure for a given nonlinear system, it is convenient to change the model to a multilinear variant form with an arbitrary seed solution and then extend the Hirota's two-soliton solution to a general variable separation ansatz. Finally, by substituting the variable separation ansatz to the original model and selecting the seed solution appropriately, one may find some nontrivial variable separated solutions.

For concreteness and completeness to see the detailed variable separation approach, we review the procedure for the DS system [21]

$$iu_t+\frac{1}{2}(u_{xx}+u_{yy})+\alpha|u|^2u-uv=0,$$
$$v_{xx}-v_{yy}-2\alpha(|u|^2)_{xx}=0, \tag{2.1}$$

with a slight modification such that we can use a same universal formula to describe all the models discussed in this paper. The DS equation is an isotropic Lax integrable extension of the well known (1+1)-dimensional nonlinear Schrödinger equation. The DS system is the shallow water limit of the Benney-Roskes equation [22,21], where u is the amplitude of a surface wave packet and v characterizes the mean motion generated by this surface wave. The DS system (2.1) can also be derived from the plasma physics [23] and from the self-dual Yang-Mills field [24]. The DS system has also been proposed as a (2+1)-dimensional model for quantum field theory [25–27]. It is known that the DS equation is integrable under some *special* meanings, say, it is IST integrable [28,29] and Painlevé integrable [30]. Many other interesting properties of the model like a special bilinear form [31], the Darboux transformation [32], finite dimensional integrable reductions [33], infinitely many symmetries [34], and the rich soliton structures [28,29,31,9,12] have also been revealed.

To find some exact solutions with some arbitrary functions of the DS equation, we make the following transformation:

$$v=v_0-f^{-1}(f_{x'x'}+f_{y'y'}+2f_{x'y'})+f^{-2}(f_{x'}^2+2f_{y'}f_{x'}+f_{y'}^2), \tag{2.2}$$
$$u=gf^{-1}+u_0,$$

with real f and complex g, where $x'=(x+y)/\sqrt{2}$, $y'=(x-y)/\sqrt{2}$ and $\{u_0,v_0\}$ is an arbitrary seed solution of the model. One may obtain the Bäcklund transformation relation (2.2) via standard truncated Painlevé expansion. Under the transformation (2.2), the DS system (2.1) is transformed to a general bilinear form,

$$(D_{x'x'}+D_{y'y'}+2iD_t)+u_0(D_{x'x'}+2D_{x'y'}+D_{y'y'})ff+2\alpha u_0gg^*+2\alpha u_0^2g^*f-2v_0gf+G_1fg=0, \tag{2.3}$$

$$2(D_{x'y'}+\alpha|u_0|^2)ff+2\alpha gh+2\alpha gfu_0^*+2\alpha u_0g^*f-G_1ff=0,$$

where D is the usual bilinear operator [35] defined as

$$D_x^mAB\equiv(\partial_x-\partial_{x_1})^mA(x)B(x_1)|_{x_1=x},$$

and G_1 is an arbitrary solution of

$$-16\alpha(u_{0x'}+u_{0y'})(u_{0x'}^*+u_{0y'}^*)+G_{1x'x'}+G_{1y'y'}+2G_{1x'y'}-4\alpha(D_{x'x'}+D_{y'y'}+2D_{x'y'})u_0u_0^*=0. \tag{2.4}$$

For the notation simplicity, we will drop the "primes" of the space variables later.

To discuss further, we fix the seed solution $\{u_0,v_0\}$ and G_1 as

$$u_0=G_1=0,\quad v_0=p_0(x,t)+q_0(y,t), \tag{2.5}$$

where $p_0\equiv p_0(x,t)$ and $q_0\equiv q_0(y,t)$ are two arbitrary functions of the indicated variables.

To solve the bilinear equation (2.3), we make the ansatz

$$f=a_0+a_1p+a_2q+a_3pq, \quad g=p_1q_1\exp(ir+is), \tag{2.6}$$

where a_0,a_1,a_2,a_3 are arbitrary constants and $p\equiv p(x,t)$, $q\equiv q(y,t)$, $p_1\equiv p_1(x,t)$, $q_1\equiv q_1(y,t)$, $r\equiv r(x,t)$, $s\equiv s(y,t)$ are all real functions of the indicated variables. If we take p, q, p_1, and q_1 as exponential functions, the variable separation ansatz reduces to the two-line soliton (or single dromion) solution form. Substituting Eq. (2.6) into Eq. (2.3) and separating the real and imaginary parts of the resulting equations, we have

$$2\Delta p_xq_y+\alpha p_1^2q_1^2=0, \tag{2.7}$$

$$\begin{aligned}&\{q_1p_{1xx}+p_1q_{1yy}-p_1q_1[2r_t+2s_t+2(p_0+q_0)+s_y^2+r_x^2]\}\\&\quad\times(a_0+a_1p+a_2q+a_3pq)+q_1(a_1+a_3q)\\&\quad\times(p_1p_{xx}-2p_{1x}p_x)+p_1(a_3p+a_2)(q_1q_{yy}-2q_{1y}q_y)=0,\end{aligned} \tag{2.8}$$

$$\begin{aligned}&[-q_1(2r_xp_{1x}+2p_{1t}+p_1r_{xx})-p_1(2s_yq_{1y}+2q_{1t}+q_1s_{yy})]\\&\quad\times(a_0+a_1p+a_2q+a_3pq)+2q_1p_1(q_t+s_yq_y)\\&\quad\times(a_3p+a_2)+2q_1p_1(r_xp_x+p_t)(a_1+a_3q)=0.\end{aligned} \tag{2.9}$$

Because the functions p_0, p, p_1, and r are only functions of $\{x,t\}$ and the functions q_0, q, q_1, and s are only functions of $\{y,t\}$, the equation system (2.7), (2.8), and (2.9) can be solved by the following variable separated equations:

$$p_1=\delta_1\sqrt{-2\Delta\alpha^{-1}c_1^{-1}p_x}, \tag{2.10}$$

$$q_1=\delta_2\sqrt{c_1q_y}, \quad (\delta_1^2=\delta_2^2=1),$$

$$p_t=-r_xp_x+c_2(a_2+a_3p)^2+c_3(a_2+a_3p)-\Delta c_4, \tag{2.11}$$

$$q_t=-s_yq_y-c_4(a_1+a_3q)^2-c_3(a_1+a_3q)+\Delta c_2,$$

$$4(2r_t+r_x^2+2p_0)p_x^2+p_{xx}^2-2p_{xxx}p_x+c_5p_x^2=0, \tag{2.12}$$

$$4(2s_t+s_y^2+2q_0)q_y^2+q_{yy}^2-2q_yq_{yyy}-c_5q_y^2=0.$$

For any fixed p_0 and q_0, solving the equation system (2.11) and (2.12) is very difficult. However, because of the arbitrariness of p_0 and q_0, we can treat the problem alternatively. Actually, we can consider the functions p and q as arbitrary functions while p_0 and q_0 are determined by Eq. (2.12) and r and s are fixed by Eq. (2.11). Consequently, the exact variable separation solution of the DS equation has the form

$$u=\frac{\delta_1\delta_2\sqrt{-2\Delta\alpha^{-1}p_xq_y}\exp(ir+is)}{a_0+a_1p+a_2q+a_3pq},$$

$$v=p_0+q_0-\frac{[(a_2+a_3p)q_{yy}+(a_1+a_3q)p_{xx}]}{a_0+a_1p+a_2q+a_3pq} \tag{2.13}$$

$$+\frac{(a_2+a_3p)^2q_y^2-2\Delta q_yp_x+(a_1+a_3q)^2p_x^2}{(a_0+a_1p+a_2q+a_3pq)^2},$$

with two arbitrary functions p and q while p_0 and q_0 are determined by Eq. (2.12) and r and s are fixed by Eq. (2.11). Especially, for the module square of the field u reads

$$|u|^2=U\alpha^{-1} \tag{2.14}$$

$$=\frac{-2^{-1}\alpha^{-1}\Delta P_xQ_y}{\left\{\sqrt{a_0a_3}\cosh\frac{1}{2}[P+Q+\ln(a_3/a_0)]+\sqrt{a_1a_2}\cosh\frac{1}{2}[P-Q+\ln(a_1/a_2)]\right\}^2}, \tag{2.15}$$

where

$$p=e^P, \quad q=e^Q, \tag{2.16}$$

and P and Q are also arbitrary functions of $\{x,t\}$ and $\{y,t\}$, respectively. In Ref. [12], a special variable separation form $(a_0=0)$ for the DS system has been given. The result of Ref. [9] is related to the special case of this paper for $p_0=q_0=a_0=0$.

From expression (2.14), we know that because the quantity expresses the value of the module square of the field u for the DS system, we have to put a constraint

$$\alpha\Delta p_xq_y<0, \tag{2.17}$$

on the selections of the functions p and q and the constants a_0, a_1, a_2, a_3, and α.

III. VARIABLE SEPARATION SOLUTIONS OF OTHER (2+1)-DIMENSIONAL MODELS

In this section, we list some known models which can be solved by means of the special variable separation approach with some suitable modifications such that they possess a common quantity expressed as Eq. (1.1).

NNV model. For the NNV model

$$u_t-au_{xxx}-bu_{yyy}+3a(uv)_x+3b(uw)_y=0, \tag{3.1}$$

$$u_x=v_y,$$

$$u_y = w_x,$$

a special variable separation solution reads

$$u = U, \tag{3.2}$$

$$v = \frac{2(a_1 + a_3 q)^2 p_x^2}{(a_0 + a_1 p + a_2 q + a_3 pq)^2} - \frac{2(a_1 + a_3 q) p_{xx}}{(a_0 + a_1 p + a_2 q + a_3 pq)} + v_0, \tag{3.3}$$

$$w = \frac{2(a_2 + a_3 p)^2 q_y^2}{(a_0 + a_1 p + a_2 q + a_3 pq)^2} - \frac{2(a_2 + a_3 p) q_{yy}}{(a_0 + a_1 p + a_2 q + a_3 pq)} + w_0, \tag{3.4}$$

where $p \equiv p(x,t)$ and $q \equiv q(y,t)$ are arbitrary functions of $\{x,t\}$ and $\{y,t\}$, respectively; a_0, a_1, a_2, and a_3 are arbitrary constants while v_0 and w_0 are related to p and q by

$$v_0 = (3ap_x)^{-1}[-p_t + ap_{xxx} + c_1 a_0 + (a_1 c_1 + a_2 c_0 + c_2 a_0) p + (a_1 c_2 + a_3 c_0) p^2], \tag{3.5}$$

$$w_0 = (3bq_y)^{-1}[-q_t + bq_{yyy} + c_0 a_0 + (a_1 c_1 + a_2 c_0 - c_2 a_0) q - (a_2 c_2 - a_3 c_1) q^2], \tag{3.6}$$

with $\{c_0, c_1, c_2\}$ being arbitrary functions of t.

In Ref. [10], a special result with $a_0 = 1$ for the NNV system had been discussed in detail. From Eq. (3.2), we know that for the NNV model (3.1), there is no constraint like Eq. (2.17) on the selections of the functions p and q and the constants a_0, a_1, a_2, and a_3.

ANNV system. The similar formula is valid for the ANNV system [36–38]

$$u_t + u_{xxx} - 3(uv)_x = 0, \quad u_x = v_y. \tag{3.7}$$

The result reads

$$u = U, \tag{3.8}$$

$$v = \frac{2(a_1 + a_3 q)^2 p_x^2}{(a_0 + a_1 p + a_2 q + a_3 pq)^2} - \frac{2(a_1 + a_3 q) p_{xx}}{(a_0 + a_1 p + a_2 q + a_3 pq)} + v_0. \tag{3.9}$$

In this case, the function $p \equiv p(x,t)$ is still an arbitrary function of $\{x,t\}$ when v_0 is fixed by

$$v_0 = -(3p_x)^{-1}[-p_t - p_{xxx} + c_1 a_0 + (a_1 c_1 + a_2 c_0 + c_2 a_0) p + (a_1 c_2 + a_3 c_0) p^2]. \tag{3.10}$$

However, the function $q = q(y,t)$ now is not an arbitrary function and should be determined by the following Riccati equation

$$-q_t + c_0 a_0 + (a_1 c_1 + a_2 c_0 - c_2 a_0) q - (a_2 c_2 - a_3 c_1) q^2 = 0, \tag{3.11}$$

where $\{c_0, c_1, c_2\}$ are arbitrary functions of t and a_0, a_1, a_2, and a_3 are arbitrary constants. If we select the functions c_0, c_1, and c_2 as

$$c_0 = \frac{1}{a_0 A_1}(A_1 A_{2t} - A_2 A_{1t} - A_2^2 A_{3t}), \tag{3.12}$$

$$c_1 = \frac{1}{a_0 A_1 \Delta}[a_2^2 A_1 A_{2t} - a_2(a_0 + a_2 A_2) A_{1t} - (a_0 + a_2 A_2)^2 A_{3t}], \tag{3.13}$$

and

$$c_2 = \frac{1}{a_0 A_1 \Delta}[a_2 a_3 A_1 A_{2t} - a_3(a_0 + a_2 A_2) A_{1t} - (a_0 a_1 + a_2 a_3 A_2^2 + 2 a_0 a_3 A_2) A_{3t}], \tag{3.14}$$

then the Riccati equation (3.11) has a solution

$$q = \frac{A_1}{A_3 + F} + A_2, \tag{3.15}$$

where $A_1 \equiv A_1(t)$, $A_2 \equiv A_2(t)$, $A_3 \equiv A_3(t)$, and $F \equiv F(y)$ are arbitrary functions of the indicated variables.

In Ref. [11], some types of special stable localized excitations with $a_0 = 1$ for the ANNV system have been obtained by selecting the arbitrary functions appropriately. For the ANNV system there is no constraint like Eq. (2.17) also.

Dispersive long wave equation system. The (2+1)-dimensional dispersive long wave equation system,

$$\begin{aligned} &u_{yt} + \eta_{xx} + u_x u_y + u u_{xy} = 0, \\ &\eta_t + u_x + \eta u_x + u \eta_x + u_{xxy} = 0, \end{aligned} \tag{3.16}$$

was first obtained by Boiti *et al.* [39] as a compatibility condition for a "weak" Lax pair. In Ref. [40], Paquin and Winternitz showed that the symmetry algebra of (1) and (2) is infinite-dimensional and has a Kac-Moody-Virasoro structure. Some special similarity solutions are also given in Ref. [40] by using symmetry algebra and the classical theoretical analysis. The more general symmetry algebra, W_∞ symmetry algebra, is given in Ref. [41]. In Ref. [42], Lou gave out nine types of two dimensional similarity reductions and thirteen types of ordinary differential equation reductions. Though the model equation system is Lax or IST integrable, it does not pass the Painlevé test [43].

For the (2+1)-dimensional dispersive long wave system, there is a special variable separation solution in the form

$$v \equiv \eta + 1 = -U, \tag{3.17}$$

$$u = \pm \frac{2 p_x (a_1 + a_3 q)}{a_0 + a_1 p + a_2 q + a_3 pq} + u_0, \tag{3.18}$$

with p being an arbitrary function of $\{x,t\}$, $q = q(y,t)$ being a solution of the Riccati equation

$$q_t - a_0 c_0 - (a_1 c_1 + a_2 c_0 - a_0 c_2) q - (a_3 c_1 - a_2 c_2) q^2 = 0, \tag{3.19}$$

and

$$u_0 = -p_x^{-1}[p_t \pm p_{xx} - a_0 c_1 - (a_1 c_1 + a_2 c_0 + a_0 c_2) p - (a_1 c_2 + a_3 c_0) p^2], \tag{3.20}$$

without the constraint like Eq. (2.17).

$(N+M)$-component AKNS system. In this subsection we write the variable separation result for a generalized $(N+M)$-component (2+1)-dimensional AKNS system,

$$\begin{aligned} & i p_{it} + p_{ixx} + p_i u_x = 0, \quad i = 1,2,\ldots,N, \\ & -i q_{jt} + q_{jxx} + q_j u_x = 0, \quad j = 1,2,\ldots,M, \\ & u_y + \sum_{i=1}^{N} \sum_{j=1}^{M} a_{ij} p_i q_j = 0, \end{aligned} \tag{3.21}$$

which was first obtained from the inner parameter dependent symmetry constraints of the Kadomtsev-Petviashvili (KP) equation [34]. In Ref. [19], the Painlevé integrability of Eq. (3.21) was confirmed. The Kac-Moody-Virasoro type algebra and the related finite transformation are obtained and the similarity partial differential equation reductions and ordinary differential equation reductions have been given by the Lie group approach [44] and the direct method [45].

The variable separation solution of the general AKNS system (3.21) possesses the form

$$p_i = \frac{P_i}{f}, \quad q_j = \frac{Q_j}{f}, \quad u = \frac{2 f_x}{f} + u_0, \tag{3.22}$$

with

$$f = a_0 + a_1 p(x,t) + a_2 q(y,t) + a_3 p(x,t) q(y,t), \tag{3.23}$$

$$P_i = F_{1i}(x,t) G_{1i}(y,t) \exp[i R_{1i}(x,t) + i S_{1i}(y,t)], \tag{3.24}$$

$$Q_j = F_{2j}(x,t) G_{2j}(y,t) \exp[-i R_{2j}(x,t) - i S_{2j}(y,t)], \tag{3.25}$$

$$G_{1i} = \frac{b_{1i}}{a_{1i}(t)} \sqrt{q_y}, \quad G_{2j} = \frac{b_{2j}}{a_{2j}(t)} \sqrt{q_y}, \tag{3.26}$$

$$F_{1i} = a_{1i}(t) \sqrt{p_x}, \quad F_{2j} = a_{2j}(t) \sqrt{p_x}, \tag{3.27}$$

$$S_{1i} = B + s_{1i}(y), \quad S_{2j} = B + s_{2j}(y), \tag{3.28}$$

$$R_{1ix} = R_{2jx} \equiv R_x = \frac{1}{2\Delta p_x}(a_2^2 \alpha_0 - \Delta p_t + a_2 \alpha_2 p + \alpha_1 p^2), \tag{3.29}$$

$$\begin{aligned} u_{0x} = \frac{1}{4\Delta^2 p_x^2} \{ & \Delta^2 p_t^2 - 2\Delta(a_2 \alpha_0 + a_2 \alpha_2 p + \alpha_1 p^2) p_t \\ & + \Delta^2 [p_{xx}^2 - 2 p_x p_{xxx} + 4 p_x^2 (B_t + R_t)] \\ & + (a_2 \alpha_2 p + a_2^2 \alpha_0 + p^2 \alpha_1)^2 \}, \end{aligned} \tag{3.30}$$

$$\begin{aligned} q_t = \frac{1}{\Delta^2} \{ & q^2 (a_3^3 \alpha_0 - a_3 \alpha_2 + \alpha_1) - q[(a_0 a_3 + a_1 a_2) \\ & \times \alpha_2 - 2 a_0 \alpha_1 - 2 a_1 a_2 a_3 \alpha_0] - a_0 a_1 a_2 \alpha_2 \\ & + a_0^2 \alpha_1 + a_1^2 a_2^2 \alpha_0 \}, \end{aligned} \tag{3.31}$$

where b_{1i} and b_{2j} are arbitrary constants and $p(x,t)$, $a_{1i}(t)$, $a_{2j}(t)$, $s_{1i}(y)$, $s_{2j}(y)$, $B \equiv B(t)$, $\alpha_0 \equiv \alpha_0(t)$, $\alpha_1 \equiv \alpha_1(t)$, $\alpha_2 \equiv \alpha_2(t)$ are all arbitrary functions of the indicated variables with the condition

$$\sum_{i=1}^{N} \sum_{j=1}^{M} a_{ij} b_{1i} b_{2j} \exp\{i[s_{1i}(y) - s_{2j}(y)]\} = -2\Delta. \tag{3.32}$$

Hence, for the quantity $v \equiv \Sigma_{i=1}^{N} \Sigma_{j=1}^{M} a_{ij} p_i q_j$, we have

$$v = U, \tag{3.33}$$

with p being an arbitrary function of x and t and $q = q(y,t)$ satisfing the Riccati equation (3.31) without constraint like Eq. (2.17). In Ref. [19], the detailed procedure to derive the variable separation solution with $a_0 = 0$ has been given.

AKNS, ADS and long wave-short wave interaction systems. The simplest case, a special AKNS system,

$$\begin{aligned} & i\psi_t + \psi_{xx} + \psi u_x = 0, \\ & -i\phi_t + \phi_{xx} + \phi u_x = 0, \\ & u_y = \phi\psi, \end{aligned} \tag{3.34}$$

is related to the $(N+M)$-component AKNS system (3.21) by $M = N = -a_{11} = 1$, $p_1 = \psi$, and $q_1 = \phi$ respectively. Especially, if we take $\phi = \psi^*$ further, the AKNS system (3.34) can be considered as an asymmetric form of the DS system. Some special variable separation forms of the AKNS system (3.34) and the ADS system are given in Refs. [46] and [13], respectively. As for the DS system, we have to put a further constraint,

$$U > 0, \tag{3.35}$$

on the ADS system.

If we make the variable transformations

$$\begin{aligned} & \psi(x,y,t) = L(x, y+t, t) \equiv L(x', y', t'), \\ & \psi(x,y,t) = S(x, y+t, t) \equiv S(x', y', t'), \end{aligned} \tag{3.36}$$

then the AKNS system (3.34) reduces to the so-called long wave–short wave interaction model [47]

$$i(L_{t'}+L_{y'})+L_{x'x'}+Lu_{x'}=0, \tag{3.37}$$

$$-i(S_{t'}+S_{y'})+S_{x'x'}+Su_{x'}=0,$$

$$u_y=LS.$$

Maccari system. In Ref. [48], a "new (2+1)-dimensional nonlinear system" is derived

$$iA_t+A_{xx}+LA=0,$$

$$iB_t+B_{xx}+LB=0, \tag{3.38}$$

$$L_y=(|A|^2+|B|^2)_x,$$

and Zhang, Huang, and Zheng [18] have obtained a variable separation solution of Eq. (3.38). Actually, taking $M=N=2$, $p_1=A$, $p_2=B$, $q_1=A^*$, and $q_2=B^*$, the $(N+M)$ component AKNS system (3.21) reduces to the Maccari system (3.38). The same constraint (3.35) should also be added to this model.

BKK system. The (2+1)-dimensional BKK system

$$H_{ty}-H_{xxy}+2(HH_x)_y+2G_{xx}=0, \tag{3.39}$$

$$G_t+G_{xx}+2(HG)_x=0, \tag{3.40}$$

has a special variable separation solution

$$G=-\frac{U}{2}, \tag{3.41}$$

$$H=\frac{(a_1+a_3q)p_x}{a_0+a_1p+a_2q+a_3pq}+H_0, \tag{3.42}$$

where p is an arbitrary function of $\{x,t\}$,

$$H_0=-(2p_x)^{-1}[p_t+p_{xx}-\Delta(c_1p^2-c_3p+c_2)], \tag{3.43}$$

and q satisfies the following Riccati equation:

$$q_t=c_1(a_0+a_1q)^2+c_2(a_1+a_3q)^2 +c_3(a_0+a_2q)(a_1+a_3q). \tag{3.44}$$

In summary, from the results (2.14), (3.2), (3.8), (3.17), (3.33), and (3.41), we know that the variable separation solution (1.1) is valid for many physically interesting models. For the DS and NNV models, both the functions p and q are arbitrary. For other models, only the function p is arbitrary while q should be a solution of a Riccati equation. For the DS model (the ADS model and the Maccari system) a further constraint (2.17) [Eq. (3.35)] should be satisfied.

IV. SPECIAL LOCALIZED STABLE SOLUTIONS

In this section, we list some special types of stable localized known excitations for the quantity U expressed by Eq. (1.1) via some suitable selections of the arbitrary functions. All the examples in this section are valid for the models without constraint (2.17) or (3.35). However, for the DS, ADS, and the Maccari systems, some examples [say, shown in Figs. 1(b), 1(d), 3, 4, 6, 7, 8, 9, 11, and 12] are not valid because of the constraint (2.17) or (3.35).

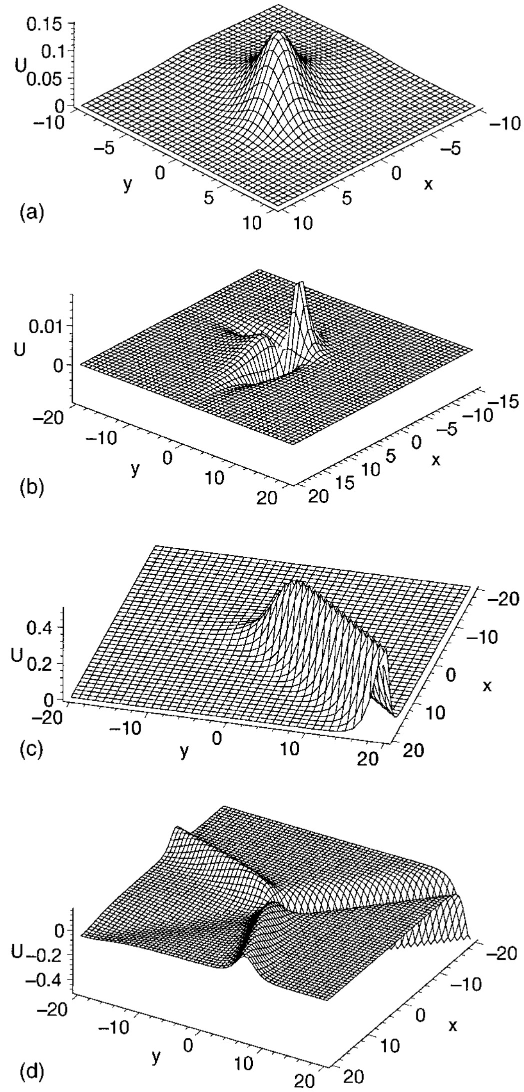

FIG. 1. Four resonant solutions driven by four straight-line soliton solutions for the quantity U shown by Eq. (1.1) with Eqs. (4.1) and (4.3) at time $t=0$. (a) The first type of a single resonant dromion with the parameters being given by Eq. (4.2). (b) The second type of single dromion solution with the condition (4.4). (c) A single solitoff solution with Eq. (4.5). (d) Four solitoff solutions under the selection (4.6). All the figures of this paper have no unit because all the models discussed in this paper are dimensionless.

Resonant dromion and solitoff solutions. If we restrict the functions p and q of Eq. (1.1) as

$$p=\sum_{i=1}^{N}\exp(k_ix+\omega_it+x_{0i})\equiv\sum_{i=1}^{N}\exp(\xi_i),$$
$$q=\sum_{i=1}^{M}\exp(K_{iy}+y_{0i})\sum_{j=1}^{J}\exp(\Omega_jt), \tag{4.1}$$

where x_{0i}, y_{0i}, k_i, ω_i, K_i, and Ω_i are arbitrary constants and M, N, and J are arbitrary positive integers, then we have a single resonant dromion solution or multiple solitoff solutions (we call a half-straight line soliton solution as a solitoff). In Fig. 1, we plot four typical structures caused by the resonant effects of four straight-line soliton solutions.

Figure 1(a) shows the structure of a first type of single resonant dromion solution shown by Eq. (1.1) with Eq. (4.1),

$$M=N=2,\quad J=k_1=K_1=1,\quad k_2=K_2=\frac{1}{3},$$
$$a_0=1,\quad a_1=a_2=3,\quad a_3=\frac{1}{2}, \tag{4.2}$$

and

$$x_{01}=y_{01}=x_{02}=y_{02}=0 \tag{4.3}$$

at $t=0$.

Figure 1(b) shows the structure of a second type of single resonant dromion solution shown by Eq. (1.1) with Eqs. (4.1), (4.3), and

$$M=N=2,\quad J=-k_1=K_1=1,\quad k_2=-K_2=\frac{1}{3},$$
$$a_0=a_2=a_3=1,\quad a_1=\frac{1}{2},\quad t=0. \tag{4.4}$$

Figure 1(c) is a plot of a single resonant solitoff solution shown by Eq. (1.1) with Eqs. (4.1), (4.3), and

$$M=N=2,\quad J=k_1=K_1=1,\quad k_2=K_2=\frac{1}{3},\quad a_0=1,$$
$$a_1=a_2=3,\quad a_3=0,\quad t=0. \tag{4.5}$$

Figure 1(d) is a plot of a four solitoff solutions shown by Eq. (1.1) with Eqs. (4.1), (4.3), and

$$M=N=2,\quad J=-k_1=K_1=1,\quad k_2=-K_2=\frac{1}{3},$$
$$a_0=a_2=3,\quad a_3=0,\quad a_1=1,\quad t=0. \tag{4.6}$$

Multidromion solutions. In the selection of Eq. (4.1), though there exist some types of single-dromion solutions with different peaks, we have not yet found a multiple dromion solution from Eq. (1.1) with Eq. (4.1). In order to obtain multiple dromion solutions, we have to change the selections of the functions p and q. For instance, if we take

$$p=\sum_{i=1}^{N} b_i \tanh^{\alpha_i}(k_i x+\omega_i t+x_{0i}) \equiv \sum_{i=1}^{N} b_i \tanh^{\alpha_i}(\xi_i),$$
$$q=\sum_{i=1}^{M} c_i \tanh^{\beta_i}(K_{iy}+y_{0i}) \sum_{j=1}^{J} \exp(\Omega_j t), \tag{4.7}$$

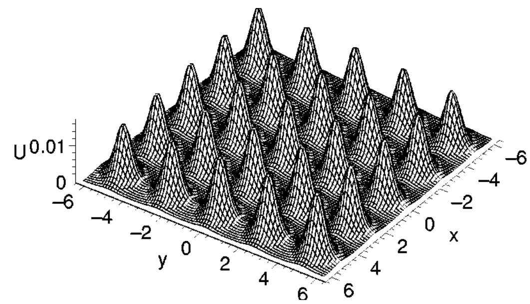

FIG. 2. A special dromion lattice solution for the quantity U expressed by Eq. (1.1) with Eqs. (4.8), (4.9), and (4.10) at time $t=0$.

where x_{0i}, y_{0i}, k_i, ω_i, K_i, β_i, b_i, c_i, α_i, and Ω_i are arbitrary constants and M, N, and J are arbitrary positive integers, then we obtain the first type of multidromion solutions.

Actually, to find multiple dromion solutions one may select the arbitrary functions p and q in quite different ways. If we change the selection (4.7) as

$$p=f(\theta),\quad \theta=\sum_{i=1}^{N} b_i \tanh^{\alpha_i}(k_i x+\omega_i t+x_{0i}),$$
$$q=g(\eta),\quad \eta=\sum_{i=1}^{M} c_i \tanh^{\beta_i}(K_{iy}+y_{0i}) \sum_{j=1}^{J} \exp(\Omega_j t), \tag{4.8}$$

where $f(\theta)$ and $g(\eta)$ are some differentiable functions of θ and η, respectively, then we obtain the second type of multidromion, dromion lattice structure. Figure 2 is a plot of a special type of dromion lattice solution with

$$f(\theta)=\exp(\theta),\quad g(\eta)=\exp(\eta), \tag{4.9}$$

and

$$M=N=5,\quad J=a_0=1, a_1=a_2=10,\quad a_3=\frac{1}{2},$$
$$k_i=K_i=2,\quad \alpha_i=\beta_i=1,\quad x_{0i}=y_{0_i}=-15+5i, \tag{4.10}$$
$$b_i=c_i=0.1,\quad i=1,2,\ldots,5,$$

when $t=0$.

Multidromion solutions driven by curved-line ghost solitons. Recently, Lou pointed out that for many (2+1)-dimensional models, a dromion may be driven not only by straight-line solitons [36] but also by curved-line solitons [37]. Actually, Eq. (2.14) shows us that the general multidromion solutions of the model expressed by Eq. (1.1) or equivalently Eq. (2.15) are driven by two sets of straight-line solitons and some curved-line solitons. The first set of straight-line solitons appears in the factor Q_y of Eq. (2.15), say, one can take

$$Q_y=\sum_{i=1}^{N} Q_i(y-y_{i0}), \tag{4.11}$$

where $Q_i = Q_i(y - y_{i0})$ denotes a straight-line soliton which is finite at the line $y = y_{i0}$ and decays rapidly away from the line. Similarly, the second set of straight-line solitons appears in the factor P_x. Finally, the curved-line solitons are determined by the factors $\sqrt{a_0 a_3}\cosh\frac{1}{2}[P+Q+\ln(a_3/a_0)]$ and $\sqrt{a_1 a_2}\cosh\frac{1}{2}[P-Q+\ln(a_1/a_2)]$ of Eq. (2.15) and the curves are determined by

$$P+Q+\ln\frac{a_3}{a_0}=\min\left|P+Q+\ln\frac{a_3}{a_0}\right|,$$
$$P-Q+\ln\frac{a_1}{a_2}=\min\left|P-Q+\ln\frac{a_1}{a_2}\right|, \tag{4.12}$$

while the number of curved-line solitons is determined by the branches of the equations in Eq. (4.12). The dromions are located at the cross points and/or the closest points of the straight and curved lines.

Multilump solutions. In high dimensions, in addition to the dromion solutions, another special type of localized structure, called lump solutions, are formed by rational functions. Actually, the multilump solutions of (2+1)-dimensional integrable models can be found by taking the arbitrary functions in many ways. Here is a special selection to find multilump solutions for the quantity U shown by Eq. (1.1),

$$p=\sum_{i=1}^{N}\frac{1}{1+(k_i x-\omega_i t-x_{i0})^2},\quad q=\sum_{i=1}^{M}\frac{1}{1+(K_i y-y_{i0})^2}. \tag{4.13}$$

Multiple oscillating dromions and lumps. If some periodic functions in space variables are included in the functions p and q of Eq. (1.1), we may obtain some types of multidromion and multilump solutions with oscillating tails. The oscillated lump solution plotted in Fig. 3(a) is related to

$$p=\frac{1}{1+\{(x-ct)[\cos(x-ct)+5/4]\}^2},\quad q=\frac{1}{1+y^2}, \tag{4.14}$$

$$a_0=a_3=1,\quad a_1=a_2=5, \tag{4.15}$$

at $t=0$ and the oscillated dromion solution in Fig. 3(b) is related to

$$p=\exp\left\{3+\sum_{i=0}^{10}\left(\frac{3}{2}\right)^{-i/2}\sin\left[\left(\frac{3}{2}\right)^{i}(k_i x+\omega_i t)\right]\right\}, \tag{4.16}$$

$$q=\exp\left\{3+\sum_{i=0}^{10}\left(\frac{3}{2}\right)^{-i/2}\sin\left[\left(\frac{3}{2}\right)^{i}(K_i x+\Omega_i t)\right]\right\}, \tag{4.17}$$

with Eq. (4.15) and

$$k_i=K_i=1,\quad t=0. \tag{4.18}$$

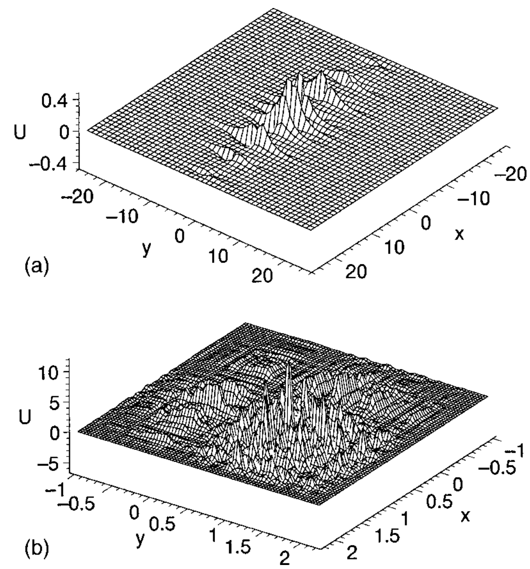

FIG. 3. (a) Plot of the special oscillating lump solution (1.1) with (4.14) and (4.15). (b) Plot of the special oscillating dromion solution (1.1) with Eqs. (4.16), (4.17), (4.15), and (4.18).

Multiple ring soliton solutions. In high dimensions, in addition to the pointlike localized coherent excitations, there may be some other types of physically significant localized excitation. For instance, in (2+1)-dimensional cases, there may be some types of ring soliton solutions which are not exactly equal to zero at some closed curves and decay exponentially away from the closed curves [49,10,11]. In Fig. 4, we plot the interaction property of a two traveling saddle type of ring solitons expressed by Eq. (1.1) with the selection

$$p=\exp\left\{-\frac{(x+20t)^4}{10\,000}+\frac{1}{5}(x+20t)+1\right\}+\exp\left\{-\frac{1}{10}(x-20t)^2+5\right\}, \tag{4.19}$$

$$q=\exp\left(\frac{y^2}{10}-5\right),\quad a_1=a_2=5,\quad a_0=a_3=0$$

at the times (a) $t=-2$, (b) $t=-0.3$, (c) $t=0$, and (d) $t=2$, respectively. Figures 4(e) and 4(f) are the contour plots of two ring solitons before the interaction (at the time $t=-1$) and after the interaction (at $t=1$), respectively. From Figs. 4(a)–4(d) and especially from Figs. 4(e) and 4(f), we can see that after head on collision of two traveling ring solitons, they preserve their shapes totally. In other words, the collision between the traveling ring solitons is completely elastic.

More concretely, to see the completely elastic interaction property between two ring solitons, we cut and move the left ring soliton of Fig. 4(d) from the center $[x=-20c_1t_0+\delta_1,\ y=\delta_2]$ (with $t_0=2$ and c_1, δ_1, and δ_2 being some suitable constants related to the possible changes of the velocity and the phase shift) to the center of the right ring soliton of Fig. 4(a) (before interaction) $[x=20t_0, y=0]$. The result single ring soliton may be described by

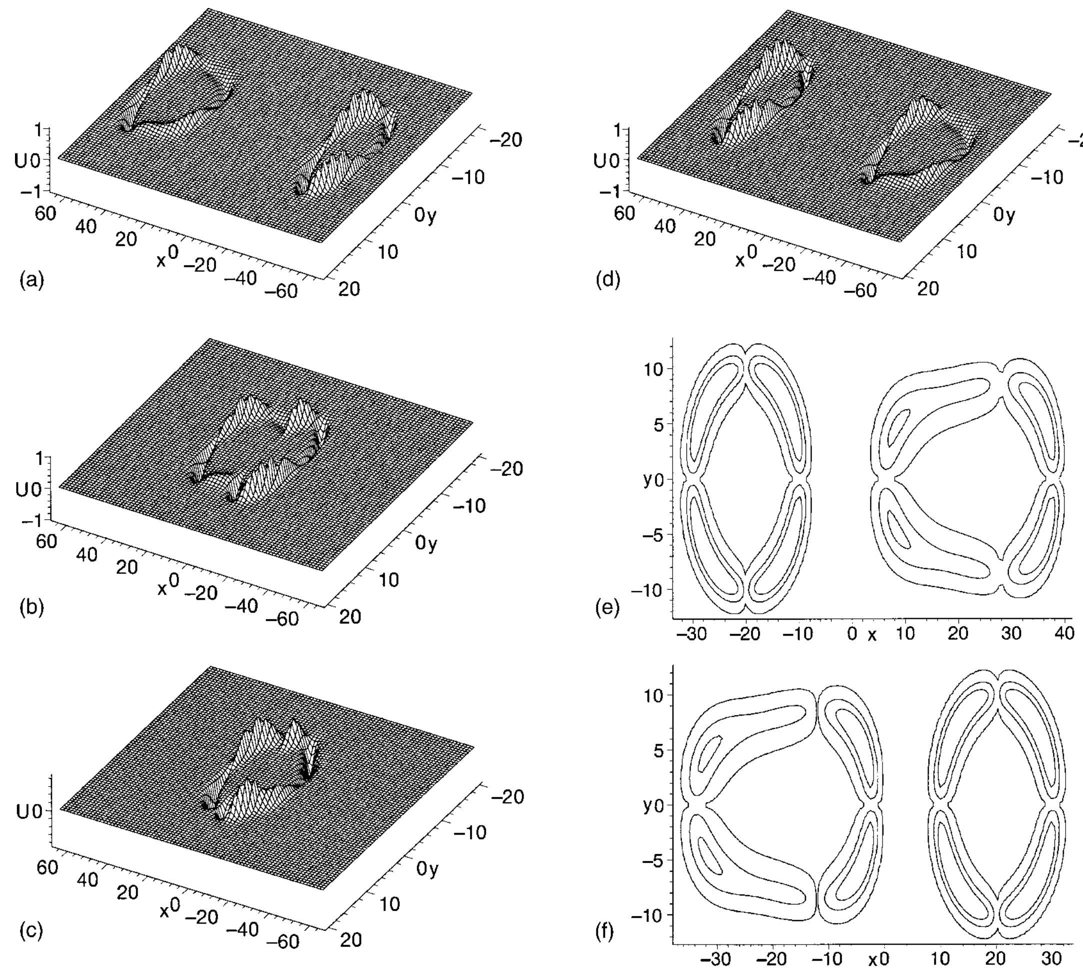

FIG. 4. Evolution plots of the two special traveling ring soliton solutions (1.1) with Eq. (4.19) at the times (a) $t=-2$, (b) $t=-0.3$, (c) $t=0$, and (d) $t=2$, respectively. (e) Contour plot of the ring solitons before collision ($t=-1$). (f) Contour plot of the ring solitons after collision ($t=1$). The values of the contours from outside to inside are $|U|=0.01,0.1,0.3$, respectively.

$$U_1 \equiv \left. \begin{Bmatrix} U(t=t_0), & x \leqslant 0 \\ 0, & x>0 \end{Bmatrix} \right|_{x\to x-20[c_1+1]t_0+\delta_1,\ \ y\to y+\delta_2}, \tag{4.20}$$

where $U(t=t_0)$ is defined by Eq. (1.1) with Eq. (4.19) and $t=t_0>0$. Similarly, we cut and move the right ring soliton of Fig. 4(d) from $[x=20c_2t_0+\delta_3, y=\delta_4]$ to the center of the left ring soliton of Fig. 4(a) $[x=-20t_0, y=0]$ and the result can be expressed as

$$U_2 \equiv \left. \begin{Bmatrix} 0, & x \leqslant 0 \\ U(t=t_0), & x>0 \end{Bmatrix} \right|_{x\to x+20[1+c_2]t_0+\delta_3,\ \ y\to y+\delta_4}. \tag{4.21}$$

Now selecting the constants c_1, c_2, δ_1, δ_2, δ_3, and δ_4 appropriately to minimize the quantity

$$v1 \equiv |U_1+U_2-U(t=-t_0)|, \tag{4.22}$$

we can find that

$$v1_{\max} \to 2\times 10^{-13} \sim 0, \tag{4.23}$$

for

$$c_1=c_2=1, \tag{4.24}$$

and

$$\delta_1=\delta_2=\delta_3=\delta_4=0. \tag{4.25}$$

The corresponding figure of Eq. (4.22) with Eqs. (4.24), (4.25), and $t_0=2$ is plotted in Fig. 5. The slight changes of the

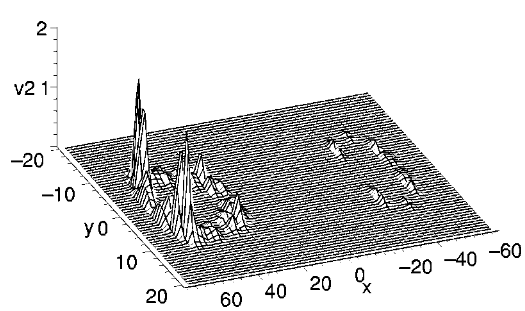

FIG. 5. Plot of the error function expressed by Eq. (4.23) with an enlargement factor 10^{13} (i.e., $v2 \equiv 10^{13} v1$) at time $t_0=2$.

parameters c_1, c_2, and δ_i, $i=1$, 2, 3, 4 will immediately lead to the rapid increase of the value of $v1$. The conclusion is true for any other $t_0>2$. The result (4.23) (i.e., $v1\sim 0$) denotes that the ring solitons preserve their shapes totally after their collision. Equation (4.24) shows us that the ring solitons preserve their velocities during the interaction. And Eq. (4.25) means that there are no phase shifts at all for the head on collision between two ring solitons. Similarly, we have studied the interaction properties for the pursue collision between two traveling ring solitons which may have the shapes different from that of Eq. (4.19). The conclusions are exactly the same.

Multibreather like soliton solutions. In (1+1)-dimensional cases, the breather solution is another type of important nonlinear excitations. Because of the arbitrariness appearing in the functions p and q of Eq. (1.1), the breather solutions of the (2+1)-dimensional models may also have quite rich structures.

In this paper, we write only one special example, multiple ring type of breathers, with the selections of the functions p and q of Eq. (1.1),

$$p=\sum_{i=1}^{N}\ \exp\{-[f_{1i}(t)x-f_{2i}(t)]^2+f_{3i}(t)\},$$
$$q=\sum_{j=1}^{M}\ \exp\{[g_{1j}(t)y]^2-g_{2j}(t)\}, \tag{4.26}$$

where $\{f_{1i}\equiv f_{1i}(t),\ f_{2i}\equiv f_{2i}(t),\ f_{3i}\equiv f_{3i}(t),\ g_{1j}\equiv g_{1j}(t),\ g_{2j}\equiv g_{2j}(t),\ i=1,2,\ldots,N,j=1,2,\ldots,M\}$ are all arbitrary periodic functions. From the expressions (1.1) and (4.26) we know that, this type of ring shaped breathers may "breathe" in some different ways. For instance, the breathers may breathe in their amplitudes (because of the periodicity of f_{1i}, g_{1i}, and f_{3i}), radius (because of the periodicity of f_{3i}/f_{1i} and g_{2j}/g_{1j}), and positions (because of the periodicity of f_{2i}). More details can be found in Fig. 6 where the corresponding parameters and functions of Eqs. (1.1) and (4.26) read

$$M=N=a_1=a_2=g_{11}=1,\ \ a_0=a_3=0,\ \ f_{31}=g_{21}=5,$$
$$f_{11}=\cos(t)+\frac{4}{3},\quad f_{21}=-20\sin(t). \tag{4.27}$$

From Figs. 6(a)–6(d), we can see that the amplitude of the ring shaped breather (1.1) with Eqs. (4.26) and (4.27) "breathes" from ~ 0.8 to ~ 6, the radius in x direction from ~ 5 to ~ 20 and the center of the ring from ~ -15 to ~ 15.

Multiple instanton solution. If some types of decaying functions of time t are included in the solution (1.1), then we can find some types of instanton solutions. For instance, the amplitude of the lump type of instanton solution (1.1) with

$$p=\frac{1}{1+x^2\,\mathrm{sech}^2 t},\quad q=\frac{2\,\mathrm{sech}^2 t}{1+y^2}, \tag{4.28}$$

$$a_0=2a_3=1,\quad a_1=a_2=10$$

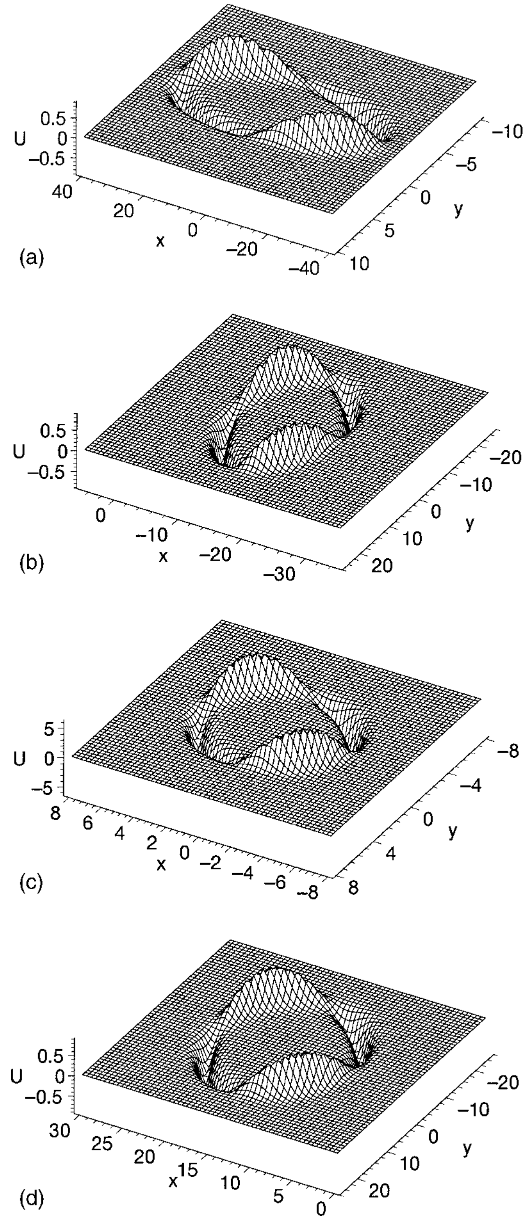

FIG. 6. Evolution plots of a special ring shape of breather solutions (1.1) with Eqs. (4.26), and (4.27) at the times (a) $t=\mp\pi$, (b) $t=-\pi/2$, (c) $t=0$, and (d) $t=\pi/2$, respectively.

will decay rapidly from $|U|\sim 0.42$ to $|U|\sim 8.4\times 10^{-5}$ as the time increases from $|t|=0$ to $|t|=5$.

V. CHAOTIC PATTERNS

Because p and q are arbitrary functions, in addition to the stable soliton selections, there may be various chaotic selections. Some interesting possible chaotic patterns are given here.

Chaotic-chaotic patterns. If we select both p and q as chaotic solutions of some (1+1)-dimensional [or (0+1)-dimensional] nonintegrable models, then the expression (1.1) becomes some types of (2+1)-dimensional space-time patterns which may be chaotic in both x and y directions. For

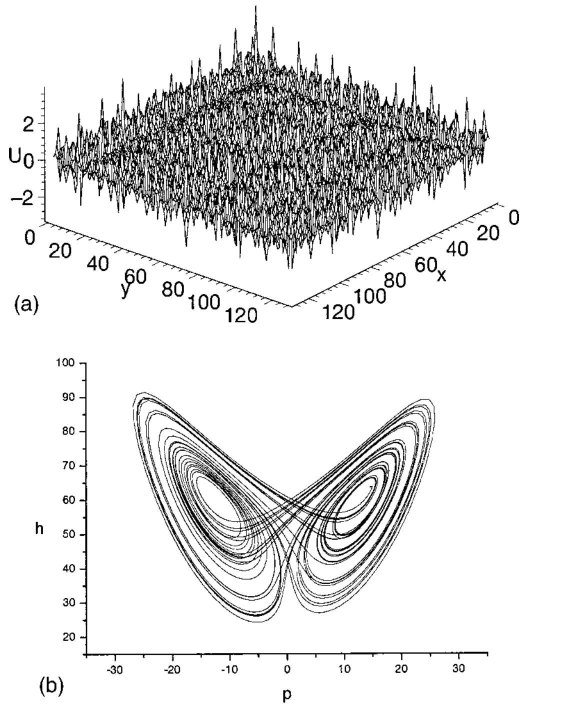

FIG. 7. (a) Plot of the chaotic-chaotic pattern (1.1) with Eq. (5.4) and the functions p and q being the chaotic solution of the Lorenz system (5.1), (5.2), and (5.5). (b) The plot of the typical chaotic solution of the Lorenz system (5.3) with Eq. (5.5).

instance, we can select p and q as the solutions of ($\tau_1 \equiv x + \omega_1 t$, $\tau_2 \equiv x + \omega_2 t$),

$$p_{\tau_1\tau_1\tau_1} = \frac{p_{\tau_1\tau_1}p_{\tau_1} + (c+1)p_{\tau_1}^2}{p} - (p^2 + bc + b)p_{\tau_1} - (b+c+1)p_{\tau_1\tau_1} + pc(ba - b - p^2), \quad (5.1)$$

$$q_{\tau_2\tau_2\tau_2} = \frac{q_{\tau_2\tau_2}q_{\tau_2} + (\gamma+1)q_{\tau_2}^2}{q} - [q^2 + \beta(\gamma+1)]q_{\tau_2} - (\beta+\gamma+1)q_{\tau_2\tau_2} + qc[\beta(\alpha-1) - q^2], \quad (5.2)$$

where ω_1, ω_2, a, b, c, α, β, and γ are all arbitrary constants. It is straightforward to prove that Eq. (5.1) [and Eq. (5.2)] is equivalent to the well-known chaos system, the Lorenz system [50],

$$p_{\tau_1} = -c(p-g), \quad g_{\tau_1} = p(a-h) - g, \quad h_{\tau_1} = pg - bh. \quad (5.3)$$

Actually, after eliminating the functions g and h in Eq. (5.3), one can find Eq. (5.1) immediately. Figure 7(a) is a special plot of a chaotic-chaotic pattern shown by Eq. (1.1) with

$$a_0 = 200, \quad a_3 = 0, \quad a_1 = a_2 = 1, \quad (5.4)$$

and p and q being given by Eqs. (5.1) and (5.2) under the following special parameter selections:

$$a = \alpha = 60, \quad b = \beta = 8/3, \quad c = \gamma = 10. \quad (5.5)$$

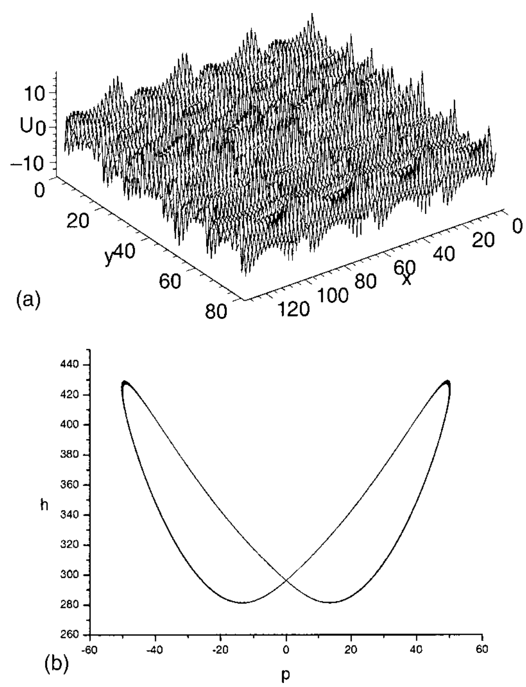

FIG. 8. (a) Plot of the chaotic-periodic pattern (1.1) with Eq. (5.4) and the functions p and q being the typical chaotic solution and periodic solution of the Lorenz systems (5.1) (with $a=60, b=8/3, c=10$) and (5.2) (with $a=350, b=8/3, c=10$), respectively. (b) The plot of the typical periodic solution of the Lorenz system (5.3) with Eq. (5.6).

Figure 7(b) is a plot for the typical chaotic solution of the Lorenz system (5.3) with Eq. (5.5).

Chaotic-periodic patterns. If we select one of p and q as a periodic function while the other one as chaotic, the solution expressed by Eq. (1.1) becomes some chaotic-periodic patterns which are chaotic in one direction and periodic in the other direction.

Figure 8(a) is a plot of a special chaotic-periodic pattern (1.1) with Eq. (5.4) and p being the chaotic solution of Eq. (5.1) with $a=60$, $b=8/3$, $c=10$, while q being the periodic solution of Eq. (5.2) with

$$\alpha = 350, \quad \beta = \frac{8}{3}, \quad \gamma = 10. \quad (5.6)$$

Figure 8(b) is a plot of the typical two-periodic solution of the Lorenz system (5.3) with Eq. (5.6).

Chaotic line soliton patterns. If one of p and q is selected as a localized function and the other one is chaotic, then the solution (1.1) becomes a chaotic line soliton.

Figure 9 is a plot of the chaotic line soliton solution expressed by Eq. (1.1) with Eq. (5.7), p being given by Eq. (5.1) with $a=60$, $b=8/3$, $c=8$, and q being given by

$$q = \tanh y. \quad (5.7)$$

Chaotic dromion patterns. In (2+1) dimensions, the most important nonlinear excitation is the dromion solution which is localized in all directions. Now the most interesting question is whether some special types of chaotic behavior can be found for the dromion excitations. Actually, the answer is

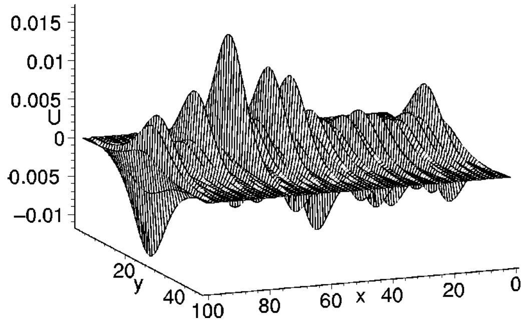

FIG. 9. Plot of the chaotic line soliton pattern (1.1) with Eq. (5.7) and p being given by Eq. (5.1) with $a=60, b=8/3, c=8$.

obviously positive because of the arbitrariness of the functions p and q. For instance, if we select p and q as $[f_2(t)>0,\ f_6(t)>0]$,

$$p=\frac{f_1(t)}{f_4(t)+\exp\{f_2(t)[x+f_3(t)]\}},$$
$$q=1+\frac{f_5(t)}{f_8(t)+\exp\{f_6(t)[y+f_7(t)]\}}, \tag{5.8}$$

with $f_i(t), i=1,2,\ldots,8$ being chaotic solutions, then Eq. (1.1) becomes a chaotic dromion which is chaotic in some different ways. The amplitude of the dromion (1.1) with Eq. (5.8) will be chaotic if $f_1(t)$, $f_4(t)$, $f_5(t)$, and/or $f_8(t)$ are chaotic. If $f_2(t)$ and/or $f_6(t)$ are chaotic, then the shape (width) of the dromion becomes chaotic. The position of the dromion located may also be chaotic if the functions $f_3(t)$ and/or $f_7(t)$ are chaotic.

In Fig. 10(a), we plot the shape of the dromion solution

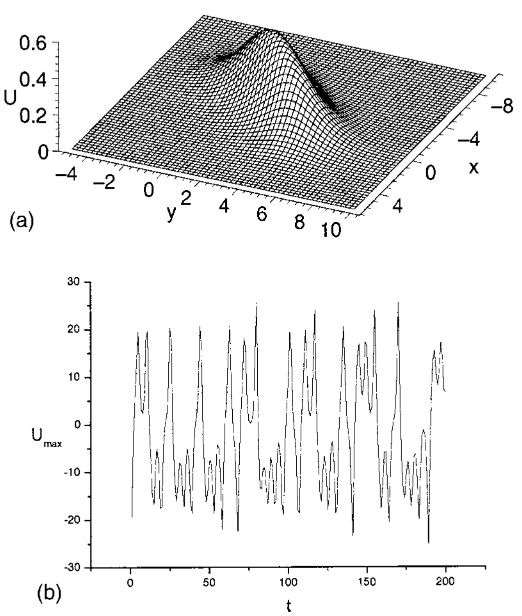

FIG. 10. (a) Plot of the single dromion solution for the quantity U given by Eq. (1.1) with Eqs. (5.7), (5.9), and $f(t)=0$. (b) The evolution of the amplitude of the chaotic dromion related to (a) with f being given by Eq. (5.10).

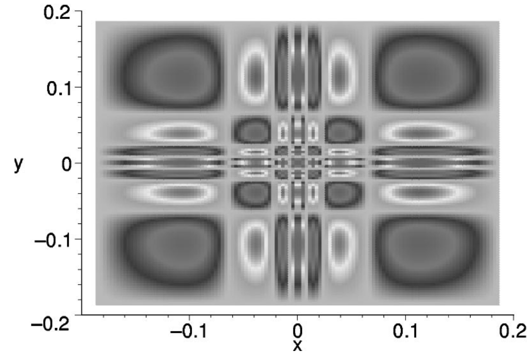

FIG. 11. Density plot of the fractal solution for the field U given by Eq. (1.1) with Eq. (6.1) at the region $\{x=[-0.185,0.185], y=[-0.185\cdots0.185]\}$ for $t=0$.

for the physical quantity U shown by Eq. (1.1) with Eq. (5.7) at a fixed time [for $f(t)=0$] with

$$p=e^{-x},\quad q=\frac{100+f(t)}{e^y+1}+1 \tag{5.9}$$

and $f(t)$ being a solution of the Lorenz system [50],

$$f_t=-10(f-g),\quad g_t=f(60-h)-g,\quad h_t=fg-\frac{8}{3}h. \tag{5.10}$$

Figure 10(b) shows the evolution of the amplitude of the dromion (1.1) with Eqs. (5.7), (5.9), and (5.10).

VI. FRACTAL PATTERNS

Recently, some types of piecewise smooth solutions like the peakons, cuspons, and compactons are widely used in (1+1)-dimensional soliton systems [51–56]. All the lower dimensional piecewise smooth functions can also be used to construct higher dimensional peakons, cuspons, and compactons. In this section and the following section we are interested in pointing out that some types of lower dimensional piecewise smooth functions with and without fractal structures can be used to construct (weak) exact solutions of higher dimensional soliton systems. In this section we list two special types of fractal patterns.

Nonlocal fractal pattern. If we select $(\xi=x+t)$,

$$p=\frac{1}{4}\xi|\xi|\{\sin[\ln(\xi^2)]-\cos[\ln(\xi^2)]\}, \tag{6.1}$$

$$q=1+\frac{1}{4}y|y|\{\sin[\ln(y^2)]-\cos[\ln(y^2)]\}, \tag{6.2}$$

in Eq. (1.1) with $a_1=a_2=1$, $a_0=a_3=0$, then we get a nonlocal exact solution with fractal structure for small $x+t$ and y. Figure 11 shows the structure of Eq. (1.1) at the region $\{x=[-0.185,0.185],\ y=[-0.185,\ldots,0.185]\}$ for $t=0$. If we plot the structure of the solution at smaller regions such as $\{x=[-0.065,0.065],\ y=[-0.065,\ldots,0.065]\}$, $\{x=[-0.0078,0.0078],\ y=[-0.0078,\ldots,0.0078]\},\ldots,$

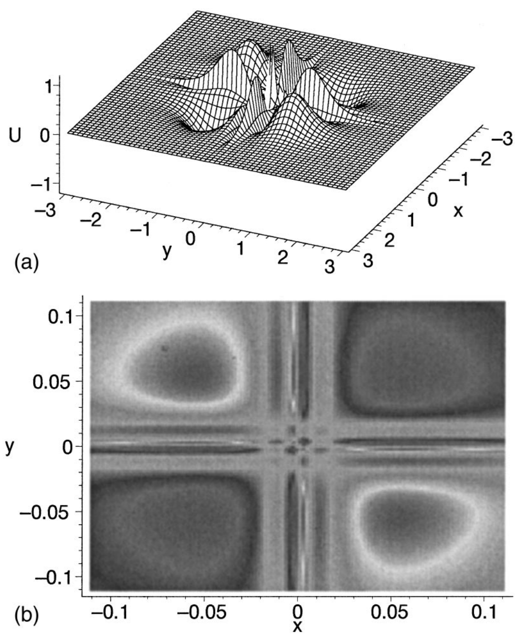

FIG. 12. Plot of the fractal dromion solution (1.1) with Eqs. (6.3), (6.4), and (6.5). (a) The localized structure of the fractal dromion. (b) The density plot of the dromion at the range $\{x=[-0.11,0.11],\ y=[-0.11,0.11]\}$. The same pictures (except the scales) can be found at infinitely many smaller ranges, say, $\{x=[-0.005,0.005],\ y=[-0.005,0.005]\}, \ldots, \{x=[-5.9\times10^{-14},\ 5.9\times10^{-14}],\ y=[-5.9\times10^{-14},\ 5.9\times10^{-14}]\}, \ldots, \{x=[-0.005,0.005],\ y=[-5.9\times10^{-14},5.9\times10^{-14}]\}, \ldots$.

$\{x=[-1.45\times10^{-10}, \ldots, 1.45\times10^{-10}],\ y=[-1.45\times10^{-10}, \ldots, 1.45\times10^{-10}]\}, \ldots,$ we can obtain totally same structures as shown in Fig. 11. Actually, to obtain the similar picture to Fig. 11, we can also use the different scales for x and y, say, $\{x=[-0.185,0.185],\ y=[-1.45\times10^{-10}, \ldots, 1.45\times10^{-10}]\}$.

Fractal dromion and lump patterns. We call a dromion (lump) solution fractal dromion (lump) if the solution is exponentially (algebraically) localized in large scale and possesses self-similar structure near the center of the dromion (lump). For instance, if we take

$$p=\exp\left\{\sqrt{(x-c_1t)^2}\left(\frac{3}{2}+\sin\{\ln[(x-c_1t)^2]\}\right)\right\}, \quad (6.3)$$

$$q=\exp\left\{\sqrt{(y-c_2t)^2}\left(\frac{3}{2}+\sin\left\{\ln\left[(y-c_2t)^2\right]\right)\right\}, \quad (6.4)$$

the expression (1.1) becomes a special fractal dromion solution.

Figure 12 is a plot of the special dromion solution (1.1) with Eqs. (6.3), (6.4), and

$$a_0=a_1=a_2=2a_3=1 \quad (6.5)$$

at time $t=0$. The localized property of the dromion is revealed in Fig. 12(a). Figure 12(b) is a density plot of the dromion solution at the range $\{x=[-0.11,0.11],\ y=[-0.11,0.11]\}$. It is interesting that by enlarging the small areas at the center of Fig. 12(b), say, $\{x=[-0.005,0.005],\ y=[-0.005,0.005]\}$, $\{x=[-0.0002,0.0002],\ y=[-0.0002,0.0002]\}, \ldots, \{x=[-5.9\times10^{-14},\ 5.9\times10^{-14}],\ y=[-5.9\times10^{-14},\ 5.9\times10^{-14}]\}, \ldots, \{x=[-0.005,0.005],\ y=[-0.0002,0.0002]\}, \ldots,$ we can find the totally same pictures as Fig. 12(b).

VII. PEAKON SOLUTIONS IN (2+1) DIMENSIONS

Since the pioneering work of Camassa and Holm (CH) [51], a special type of weak solutions of (1+1)-dimensional nonlinear evolution equations has attracted the attention of physicists and mathematicians [55]. These types of solitary waves are called peakons because they are discontinuous at their crest [51]. Especially, the properties and interaction behaviors of the peakons for (1+1)-dimensional integrable CH equation have been understood quite well. The collisions among the (1+1)-dimensional peakons are completely elastic. Though the CH equation has been extended to (2+1) dimensions in several possible ways [57], one does not know anything on the (2+1)-dimensional peakons which are localized in all directions for any (2+1)-dimensional integrable model.

In fact, the entrance of the arbitrary functions p and q in the universal quantity expressed by Eq. (1.1) tells that the (2+1)-dimensional peakons can exist at least for all the models listed in this paper by selecting the arbitrary functions as some suitable piecewise continuous functions. In this section, we give two special types of (2+1)-dimensional peakons.

The first type of peakons can be obtained by selecting one of p and q of Eq. (1.1) as a piecewise function while the other one as a continue differentiable function. For instance, we can take the function q as a continue function (say, one of those listed in the examples of the last three sections) while p is given by

$$p=\sum_{i=1}^{M}\begin{cases}F_i(x+c_it), & x+c_it\leqslant 0\\ -F_i(-x-c_it)+2F_i(0), & x+c_it>0,\end{cases} \quad (7.1)$$

where the function $F_i(\xi)\equiv F_i(x+c_i)$, $i=1,2,\ldots,M$ are differentiable functions and possess the boundary conditions

$$F_i(\pm\infty)=C_{\pm i}, \quad i=1,2,\ldots,M \quad (7.2)$$

with $C_{\pm i}$ being constants and/or ∞. The second type of peakon solutions is yielded by selecting both p and q in Eq. (1.1) as some piecewise functions. For instance, p is still given by Eq. (7.1) while q is taken as

$$q=\sum_{i=1}^{N}\begin{cases}G_i(y), & y\leqslant 0\\ -G_i(-y)+2G_i(0), & y>0,\end{cases} \quad (7.3)$$

where the functions $G_i(y)$, $i=1,\ 2,\ldots,N$ are differentiable functions and possess the boundary conditions similar to Eq. (7.2).

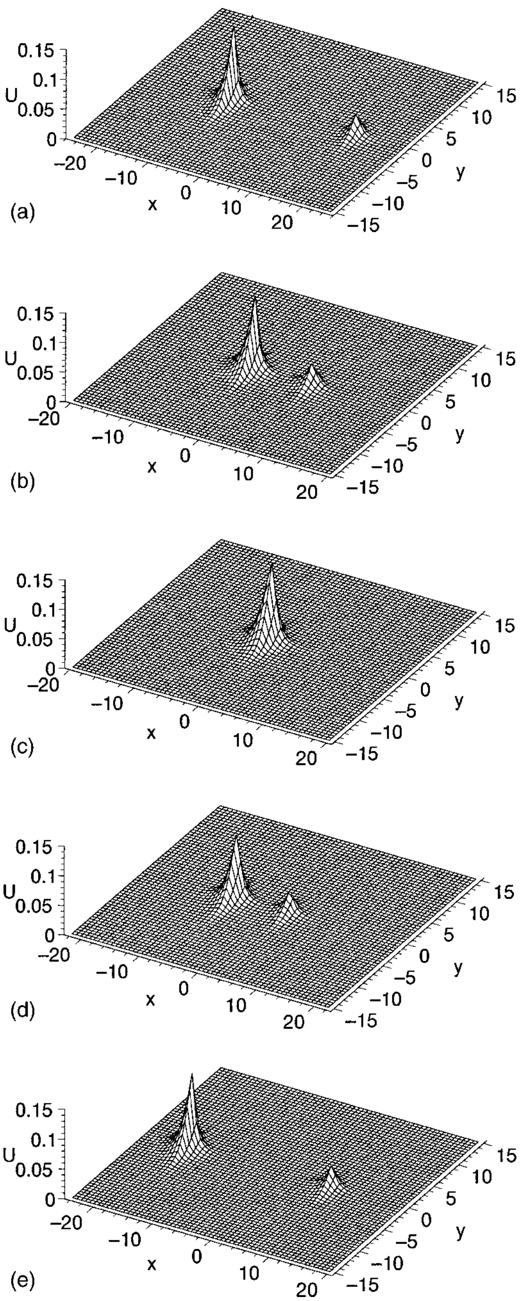

FIG. 13. Exhibition of the interaction property between two peakons shown by Eq. (1.1) with $a_0=0, a_1=a_2=2a_3=1$, Eqs. (7.4) and (7.5) at the time (a) $t=-8$, (b) $t=-3$, (c) $t=0$, (d) $t=3$, and (e) $t=8$, respectively.

In Fig. 13, we plot the interaction property between two second type of peakons for the quantity (1.1) with $a_0=0$, $a_1=a_2=2a_3=1$,

$$p=1+\begin{cases} -\ln\left\{\tanh\left[\frac{1}{2}(1-x+t)\right]\right\}, & x\leqslant t \\ \ln\left\{\tanh\left[\frac{1}{2}(1+x-t)\right]\right\}-2\ln\left[\tanh\left(\frac{1}{2}\right)\right], & x>t, \end{cases} \tag{7.4}$$

$$+\begin{cases} -\ln\left\{\tanh\left[\frac{1}{2}(1-x-2t)\right]\right\}, & x\leqslant -2t \\ \ln\left\{\tanh\left[\frac{1}{2}(1+x+2t)\right]\right\}-2\ln\left[\tanh\left(\frac{1}{2}\right)\right], & x>-2t, \end{cases}$$

and

$$q=\begin{cases} -\ln\left\{\tanh\left[\frac{1}{2}(1-y)\right]\right\}, & y\leqslant 0 \\ \ln\left\{\tanh\left[\frac{1}{2}(1+y)\right]\right\}-2\ln\left[\tanh\left(\frac{1}{2}\right)\right], & y>0. \end{cases} \tag{7.5}$$

From Fig. 13, we can see that the interactions among peakons are not completely elastic. After interaction, two peakons exchange their shapes completely and preserve their velocities. Similar to the case of the interaction of the ring solitons, to see the interaction property between the peakons more clearly, we cut and move the left peakon of Fig. 13(e) from the center $[x=-2c_1t_0+\delta_1,\ y=\delta_2](t_0=8)$ to the center of the left peakon of Fig. 13(a) $[x=-t_0, y=0]$. The resulting single peakon may be described by

$$U_1\equiv\left.\begin{cases} U(t=t_0), & x\leqslant 0 \\ 0, & x>0 \end{cases}\right\}_{x\to x-[2c_1-1]t_0+\delta_1,\ y\to y+\delta_2}, \tag{7.6}$$

where $U(t=t_0)$ is defined by Eq. (1.1) with $a_0=0$, $a_1=a_2=2a_3=1$, Eqs. (7.4) and (7.5). Similarly, we cut and move the right peakon of Fig. 13(e) from $[x=c_2t_0+\delta_3, y=\delta_4]$ to the center of the right peakon of Fig. 13(a) $[x=2t_0, y=0]$ and the result can be expressed as

$$U_2\equiv\left.\begin{cases} 0, & x\leqslant 0 \\ U(t=t_0), & x>0 \end{cases}\right\}_{x\to x-[2-c_2]t_0+\delta_3, y\to y+\delta_4}. \tag{7.7}$$

Now selecting the constants c_1, c_2, δ_1, δ_2, δ_3, and δ_4 appropriately to minimize the quantity

$$v1\equiv|U_1+U_2-U(t=-t_0)|, \tag{7.8}$$

we can find that

$$v1_{\max}\to 3\times 10^{-17}\sim 0, \tag{7.9}$$

for

$$c_1=c_2=1, \tag{7.10}$$

and

$$\delta_1=\delta_2=\delta_3=\delta_4=0. \tag{7.11}$$

The corresponding figure of Eq. (7.8) with Eqs. (7.10), (7.11), and $t_0=8$ is plotted in Fig. 14. The result (7.9) (i.e., $v1\sim 0$) indicates that the peakons exchange their shapes totally after collision. Equation (7.10) shows us that the pea-

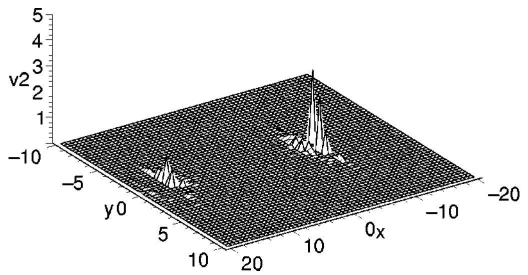

FIG. 14. Plot of an error function $v1$ expressed by Eq. (7.8) with Eqs. (7.10), (7.11), and an enlargement factor 10^{17} (i.e., $v2 \equiv 10^{17} v1$) at time $t_0 = 8$.

kons preserve their velocities after interaction. And Eq. (7.11) means that there are not phase shifts at all for the head on collision of peakons. Similarly, these conclusions hold true both for the pursue collision between two peakons and for the interactions of the first type of peakons.

VIII. SUMMARY AND DISCUSSIONS

In summary, for some (2+1)-dimensional soliton systems such as the DS equation, NNV equation, ADS equation, ANNV equation, DLWE system, BKK system, LWSW model, Maccari system, and the generalized $(N+M)$-component AKNS system, some lower dimensional arbitrary functions can be included in their exact solutions. A common variable separation formula is valid for all these models. In addition to the many types of stable localized excitations such as the solitoffs, dromions, lumps, breathers, instantons, and ring solitons, there may be many types of chaotic and fractal patterns by selecting the arbitrary functions as the chaotic and/or fractal solutions of some *lower* dimensional nonintegrable models. Especially, the dromion type solutions that are localized in all directions for some types of physical fields may also be chaotic in some different ways (say, chaotic in their amplitudes, positions, and widths). Similar to the cases in (1+1) dimensions, the weak solutions like the peakon solutions may also exist in higher dimensions. Two types of explicit peakon solutions that are localized in all directions have also been given in this paper.

For the existence of the abundant structures of the universal formula (1.1), it is quite important but difficult to investigate the interaction properties for all the possible localized excitations. In this paper, the interactions of two special types of localized traveling excitations, ring solitons and the peakons, are studied. For the traveling ring soliton solutions, the interaction is completely elastic. During the collision (both for the head on collision and the pursue collision), the ring solitons pass through each other and completely preserve their shapes, velocities, and phases. For the traveling peakons, the peakons also pass through each other with unchanged velocities and phases, however, their shapes are completely exchanged.

Why do the (2+1)-dimensional integrable models possess so rich localized excitations and why can some lower dimensional chaotic and fractal solutions enter into the higher dimensional integrable models? All the reasons come from the existence of the characteristics, arbitrary functions, in the universal formula (1.1). Actually, it is known that arbitrary exotic behaviors may propagate along the characteristics. The similar situation exists even also in linear system like the wave equation

$$u_{tt} - c^2 u_{xx} = 0. \tag{8.1}$$

It is known that there are two characteristic functions, $f(x-ct)$ and $g(x+ct)$, included linearly in the general solution of the wave equation (8.1). If one can find the general solution of the nth order $(m+1)$-dimensional nonlinear integrable models, there should be nm-dimensional characteristic functions in the general solution. Of course, these characteristics should be combined highly nonlinearly in the general solutions of nonlinear models. In our *special* variable separation solution (1.1) there exist only two characteristic functions.

Though the localized excitations such as the dromions, lumps, ring solitons, and the peakons possess zero boundary conditions for the quantity U, the boundary conditions for other quantities, say, the quantity v (2.13) for the DS model and v and w [Eqs. (3.3) and (3.4)] for the NNV system, are not exactly zero. Different selections of the functions p and q in (1.1) correspond to different selections of boundary conditions of fields (or potentials) with nonzero boundary conditions. The changes of these boundary conditions (exotic behavior) propagate along the characteristic and then yield the changes of the localized excitations. That means, in some sense, the dromions and other types of localized excitations for some physical quantities are remote controlled by some other quantities (or potentials) which have nonzero boundary conditions. In Ref. [58], by using pure numerical calculations, the authors have also pointed out that the nonchaotic dromions of the DS equation can be remote controlled.

It is also known that both the ANNV system and the DS systems are related to the KP equation [24,38], while the DS and the KP equations are the reductions of the self-dual Yang-Mills (SDYM) equation [24,38]. So both the KP and the SDYM equations may possess quite rich nonlinear excitations with some arbitrary characteristics. The KP equation is another type of important integrable model in the study of integrable models. However, we have not yet found an effective way to obtain its nontrivial variable separation solutions. In our special variable separation expression (1.1), there are only two characteristic functions. How to introduce more characteristic functions into the variable separation solutions is also an essential open question. These interesting and important problems should be studied further.

ACKNOWLEDGMENTS

The authors thank Professors Q. P. Liu, Professor X. B. Hu, Professor C. P. Sun, Professor Y. S. Li, Professor G. X. Huang, Dr. C.-l. Chen, Dr. S.-l. Zhang, Dr. X.-m. Qian, and Dr. B. Wu for helpful discussions. The work was supported by the National Outstanding Youth Foundation of China (Grant No. 19925522), the Research Fund for the Doctoral Program of Higher Education of China (Grant No. 2000024832), and the Natural Science Foundation of Zhejiang Province of China.

[1] G. I. Stegeman and M. Segev, Science **286**, 1518 (1999); Y. S. Kivshar and B. A. Malomend, Rev. Mod. Phys. **61**, 763 (1989); A. G. Abanov and P. B. Wiegmann, Phys. Rev. Lett. **86**, 1319 (2001); Q. P. Liu and M. Manas, Phys. Lett. A **239**, 159 (1998); X. B. Hu and H. W. Tam, *ibid.* **276**, 30 (2000); G. X. Huang, S. D. Zhang, and B. B. Hu, Phys. Rev. B **58**, 9194 (1998).

[2] J. P. Gollub and M. C. Cross, Nature (London) **404**, 710 (2000); R. A. Jalabert and H. M. Pastawski, Phys. Rev. Lett. **86**, 2490 (2001); M. van Hecke and M. Howard, *ibid.* **86**, 2018 (2001); G. Hu, Y. Zhang, H. A. Cerdeira, and S. G. Chen, *ibid.* **85**, 3377 (2000).

[3] D. Bonamy, F. Daviaud, L. Laurent, M. Bonetti, and J. P. Bouchaud, Phys. Rev. Lett. **89**, 034301 (2002); K. S. S. Wu, O. Lahav, and M. J. Rees, Nature (London) **397**, 225 (1999); J. W. Kirchner, X. H. Feng, and C. Neal, Nature (London) **403**, 524 (2000).

[4] J. Eilbeck (unpublished).

[5] S.-y. Lou and X.-y. Tang, Q.-P. Liu, and T. Fukuyama, Z. Naturforsch (to be published); e-print nlin.SI/0108045 2001; X.-y. Tang and H.-c. Hu, Chin. Phys. Lett. **9**, 1225 (2002).

[6] S.-y. Lou and L.-l. Chen, J. Math. Phys. **40**, 6491 (1999).

[7] Y. Cheng and Y.-s. Li, Phys. Lett. A **175**, 22 (1991); B. G. Konopelchenko, J. Sidorenko, and W. Strampp, *ibid.* **175**, 17 (1991).

[8] C.-w. Cao, Sci. China, Ser. A: Math., Phys., Astron. Technol. Sci. **33**, 528 (1990).

[9] S.-y. Lou and J.-Z. Lu, J. Phys. A **29**, 4029 (1996).

[10] S.-y. Lou, Phys. Lett. A **277**, 94 (2000).

[11] S.-y. Lou and H.-y. Ruan, J. Phys. A **34**, 305 (2001).

[12] S.-y. Lou, Phys. Scr. **65**, 7 (2000).

[13] H.-y. Ruan and Y.-x. Chen, Acta Phys. Sin. **4**, 586 (2001), in Chinese.

[14] X.-y. Tang and S.-y. Lou, Chaos, Solitons Fractals **14**, 1451 (2002); X.-y. Tang, C.-l. Chen, and S.-y. Lou, J. Phys. A **35**, L293 (2002).

[15] J.-p. Ying and S.-y. Lou, Z. Naturforsch., A: Phys. Sci. **56**, 619 (2001); H.-m. Li and S.-y. Lou (unpublished).

[16] X.-y. Tang and S.-y. Lou, Commun. Theor. Phys. **38**, 1 (2001).

[17] W.-h. Huang and J.-F. Zhang, Chin. Phys. (to be published).

[18] J. Zhang, W. Huang, and C. Zheng, Acta Phys. Sin. (to be published).

[19] S.-y. Lou, C.-l. Chen, and X.-y. Tang, J. Math. Phys. **43**, 4078 (2002).

[20] S.-y. Lou, X.-y. Tang, and Y. Zhang, e-print nlin.PS/0107029.

[21] A. Davey and K. Stewartson, Proc. R. Soc. London, Ser. A **338**, 101 (1974).

[22] D. J. Benney and G. J. Roskes, Stud. Appl. Math. **47**, 377 (1969).

[23] K. Nishinari, K. Abe, and J. Satsuma, J. Phys. Soc. Jpn. **62**, 2021 (1993).

[24] M. J. Ablowitz and P. A. Clarkson, *Solitons, Nonlinear Evolution Equations and Inverse Scattering*, London Mathematical Society Lecture Note Series 149 (Cambridge University Press, Cambridge, England, 1991).

[25] C. L. Schultz, M. J. Ablowitz, and D. BarYaacov, Phys. Rev. Lett. **59**, 2825 (1987).

[26] P. P. Kulish and V. D. Lipovsky, Phys. Lett. A **127**, 413 (1988).

[27] G. D. Pang, F. C. Pu, and B. H. Zhao, Phys. Rev. Lett. **65**, 3227 (1990).

[28] M. Boiti, J. J. P. Leon, L. Martina, and F. Penpinelli, Phys. Lett. A **132**, 432 (1988).

[29] A. S. Fokas and P. M. Santini, Phys. Rev. Lett. **63**, 1329 (1989); Physica D **44**, 99 (1990).

[30] R. A. Leo, G. Mancarella, G. Soliani, and L. Solombrino, J. Math. Phys. **29**, 2666 (1988).

[31] J. Hietarinta, Phys. Lett. A **149**, 133 (1990).

[32] V. B. Matveev and M. A. Salle, *Darboux Transformations and Solitons* (Springer-Verlag, Berlin, 1991).

[33] Z.-x. Zhou, Inverse Probl. **12**, 89 (1996); **14**, 1371 (1998); Z.-x. Zhou and W.-x. Ma, J. Phys. Soc. Jpn. **70**, 1241 (2001).

[34] S.-y. Lou and X.-b. Hu, J. Phys. A **27**, L207 (1994).

[35] R. Hirota, Phys. Rev. Lett. **27**, 1192 (1971).

[36] M. Boiti, J. J. P. Leon, M. Manna, and F. Penpinelli, Inverse Probl. **2**, 271 (1986).

[37] S.-y. Lou, J. Phys. A **28**, 7227 (1995); **29**, 5989 (1996).

[38] S.-y. Lou and X.-b. Hu, J. Math. Phys. **38**, 6401 (1997).

[39] M. Boiti, J. J. P. Leon, and F. Pempinelli, Inverse Probl. **3**, 371 (1987).

[40] G. Paquin and P. Winternitz, Physica D **46**, 122 (1990).

[41] S.-y. Lou, J. Phys. A **27**, 3235 (1994).

[42] S.-y. Lou, Math. Methods Appl. Sci. **18**, 789 (1995).

[43] S.-y. Lou, Phys. Lett. A **176**, 96 (1993).

[44] P. J. Olver, *Application of Lie Groups to Differential Equation*, 2nd ed., Graduate Texts Mathematics Vol. 107 (Springer, New York, 1993); G. W. Bluman and S. Kumei, *Symmetries and Differential Equation*, Applied Mathematical Science Vol. 81 (Springer, Berlin, 1989).

[45] P. A. Clarkson and M. D. Kruskal, J. Math. Phys. **30**, 2201 (1989); S. Y. Lou, Phys. Lett. A **151**, 133 (1990); P. A. Clarkson, J. Phys. A **22**, 2355 (1989); **22**, 3821 (1989); Chaos, Solitons Fractals **5**, 2261 (1995); E. Pucci, J. Phys. A **25**, 2631 (1992); **26**, 681 (1993); G. Saccomandi, *ibid.* **30**, 2211 (1997); S.-y. Lou, X.-y. Tang, and J. Lin, J. Math. Phys. **41**, 8286 (2000).

[46] S.-y. Lou, J. Lin, and X.-y. Tang, Eur. Phys. J. B **22**, 473 (2001).

[47] M. Oikawa, M. Okamura, and M. Funakoshi, J. Phys. Soc. Jpn. **58**, 4416 (1989); M. Boiti, J. Leon, L. Matina, and F. F. Pempinelli, Phys. Lett. A **132**, 432 (1988).

[48] A. Maccari, J. Phys. A **38**, 4151 (1997); A. Uthayakumar, K. Nakkeran, and K. Porsezia, Chaos, Solitons Fractals **10**, 1513 (1999); J. F. Zhang, Commun. Theor. Phys. **35**, 267 (2001); D. W. C. Lai and K. W. Chow, J. Phys. Soc. Jpn. **70**, 666 (2001).

[49] S.-y. Lou, J. Math. Phys. **41**, 6509 (2000).

[50] F. W. Lorenz, J. Atmos. Sci. **20**, 130 (1963); M. Clerc, P. Coullet, and E. Tirapegui, Phys. Rev. Lett. **83**, 3820 (1999).

[51] R. Camassa and D. D. Holm, Phys. Rev. Lett. **71**, 1661 (1993).

[52] F. Calogero, A. Degasperis, and X.-d. Ji, J. Math. Phys. **41**, 6399 (2000); **42**, 2635 (2001).

[53] A. Maccari, J. Math. Phys. **37**, 6207 (1996); **38**, 4151 (1997); **40**, 3971 (1999); **42**, 2689 (2001).

[54] F. Calogero and M. C. Nucci, J. Math. Phys. **32**, 72 (1991).

[55] T. Qian and M. Tang, Chaos, Solitons Fractals **12**, 1347 (2001); R. A. Kraenkel, M. Senthilvelan, and A. I. Zenchunk,

Phys. Lett. A **273**, 183 (2000).

[56] P. Rosenau, Phys. Rev. Lett. **73**, 1737 (1994); P. Rosenau and J. M. Hyman, *ibid.* **70**, 564 (1993); S. Y. Lou and Q. X. Wu, Phys. Lett. A **262**, 344 (1999).

[57] D. D. Holm, J. E. Marston, and T. S. Ratiu, Adv. Math. **137**, 1 (1998).

[58] N. Yoshida, K. Nishinari, J. Satsuma, and K. Abe, J. Phys. A **31**, 3325 (1998).